SATURNUS: The UCLA Infrared Free-Electron Laser Project

J.W. Dodd, S.C. Hartman, S. Park, C. Pellegrini, J.B. Rosenzweig, J.A. Smolin, G. Hairapetian, J. Kolonko, W.A. Barletta, D.B. Cline
Center for Advanced Accelerators, Department of Physics, U.C.L.A., Los Angeles, CA, 90024-1547

J.G. Davis, C.J. Joshi, N.C. Luhmann Jr.
Department of Electrical Engineering, U.C.L.A., Los Angeles, CA 90024-1594

S.N. Ivanchenkov, A.S. Khlebnikov, Yu.Yu. Lachin, A.A. Varfolomeev
I.V. Kurchatov Institute of Atomic Energy, Moscow, 123182, U.S.S.R

ABSTRACT: A compact 20 MeV linac with an RF laser-driven electron gun will be used to drive a high-gain (10cm gain length), 10.6μm wavelength FEL amplifier, operating in the SASE mode. Saturnus will mainly study FEL physics in the high-gain regime, including start-up from noise, optical guiding, sidebands, saturation, and superradiance, with emphasis on the effects important for future short wavelength operation of FEL's. The hybrid undulator was designed and built at the Kurchatov Institute of Atomic Energy in the U.S.S.R. The primary magnetic flux is provided by C-shaped iron yokes, where between the poles thin blocks of neodymium-iron-boron magnets are placed to provide additional magnetic flux along the undulator axis. The field strength is adjusted by moving the thin Nd-Fe-B blocks on a set-screw mount. The initial assembly will have forty periods, each 1.5cm long. The gap distance between the "yoke" pole-pieces is fixed at 5mm. The undulator field has been measured, yielding an on axis peak value of 6.6kGauss, which closely matches computer simulations.

Table 1. Saturnus design parameters.

ELECTRON BEAM	
Energy, nominal	16.5MeV
Energy spread, r.m.s.	0.2%
Peak current	200A
Klystron frequency	2.865GHz
Pulse repetition rate	5Hz
Macropulse duration	3.5μsec
micropulse duration, r.m.s.	≈1.6psec
Charge per bunch	≈1nC
Normalized emittance, r.m.s.	8mm-mrad
UNDULATOR	
Drift tube I.D. within undulator	4mm
Electron beam diameter in undulator	0.4mm
Period	1.5cm
Length	60cm
Fixed gap between pole pieces	5mm
Field on axis	6.6kGauss
FEL OUTPUT RADIATION	
Wavelength	10.6μm
Gain length	10cm
Saturation length	130cm
Peak saturated power	50MW

ACKNOWLEDGEMENTS: Our group appreciates the help received from H. Kirk, K. Batchelor, J. Xie, J. Sheehan, G. Bennett, J. Wurtele, M. Allen, G. Loew, M. Baltay, and H. Hoag. This work is supported by DOE Grant No. DOE-DE-AS-3-90ER-40583.

I. INTRODUCTION

A compact 16.5 MeV linac with an RF laser-driven electron gun[1] is being built at UCLA (See S.C. Hartman, *et al.*, this Conf.). This linac will be used to study the production of high-brightness electron beams, and to drive a high gain, 10.6μm wavelength FEL amplifier, capable of operating in the SASE mode. Saturnus will use a 1.5cm period, 6.6kG peak field undulator developed and built at the I.V. Kurchatov Institute of Atomic Energy. Table 1 shows beam parameters.

Saturnus will mainly study FEL physics in the high-gain regime, including start-up from noise, optical guiding, sidebands, saturation, and superradiance, with emphasis on the effects important for future short wavelength operation of FEL's.[2] For the electron beam we will study ways to improve the beam brightness and peak current. We will have two beam lines, one leading straight into the undulator, the other designed for beam diagnostic and longitudinal bunch compression. This second beam line will also be used for other particle beam physics experiments, including plasma wakefield acceleration.[3]

II. FEL OUTPUT: SIMULATIONS AND DIAGNOSIS

The FEL performance in SASE is evaluated using the TDA code developed by Tran and Wurtele at MIT.[4] TDA predicts a gain length of 10cm, with a saturation power of 50MW. This assumes that a full 200A peak current is achievable. Fig. 1(a) graphs the power versus distance along the undulator as projected by TDA. Fig. 1 uses an input power of 40mW, corresponding to the spontaneous radiation emitted in one gain length, within an angle $\Theta = 1/(\Upsilon\cdot\sqrt{N})$ and a line width 1/(2N). This radiation is assumed to be focused to a spot radius $(\lambda L_{UNDUL.})^{1/2}/4\pi$ at the centre of the first gain length.

Fig. 1(b) plots the calculated r.m.s. optical beam radius versus the distance along the undulator. Notice that once growth occurs the optical beam collapses and remains in the vicinity of the electron beam as it propagates down the entire undulator. It is interesting to note that the optical beam radius and the gain length depend on the extent of detuning the electron beam energy from the resonant energy.

The FEL's output wavelength will closely match the 10.6μm radiation which CO_2 lasers produce, simplifying the diagnosis of the output radiation by allowing the possibility to inject the FEL with an external CO_2 laser. For cryogenic

0-7803-0135-8/91$01.00 ©IEEE

infrared detectors sensitive to 10μm wavelengths, the expected power output from spontaneous emission in the FEL (excluding gain) is marginally detectable. For 1nC charge per bunch, $1.2 \cdot 10^7$ photons per micropulse are expected from spontaneous emission within the angle and linewidth given above over a 10cm distance. For smaller charges one may need to integrate the signal over many pulses. As seen from fig. 1(a) at the end of the undulator section, roughly 3kW of power occurs from exponential gain. This power level corresponds to 10^{12} photons per micropulse and is easily detected.

III. HYBRID UNDULATOR

The hybrid undulator was designed and constructed at the Kurchatov Institute of Atomic Energy in the U.S.S.R. The primary magnetic flux is provided by $SmCo_5$ magnets placed in the middle of C-shaped vanadium-permendur yokes. Thin blocks of neodymium-iron-boron magnets are placed between the poles to provide additional magnetic flux. The field strength is adjusted by moving the thin Nd-Fe-B blocks towards or away from the axis on a set-screw mount. Fig. 2 is a schematic diagram of the Kurchatov undulator. The initial assembly has forty periods, each period being 1.5 cm long. The gap distance between the "yoke" pole-pieces is fixed at

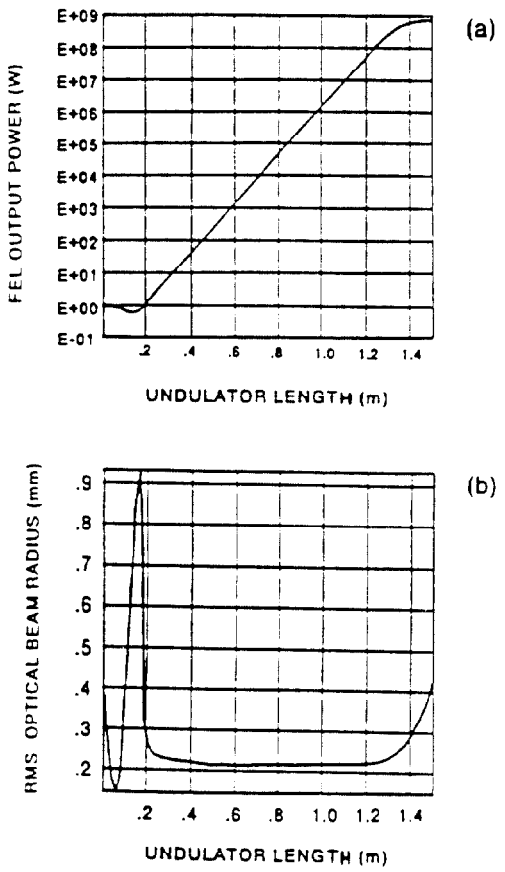

Figure 1. TDA simulations of SASE using the parameters in table 1: (a) power growth through the undulator and (b) radius of the optical beam within the undulator. Optical guiding is evident since the optical beam remains confined near the electron beam, once power growth predominates.

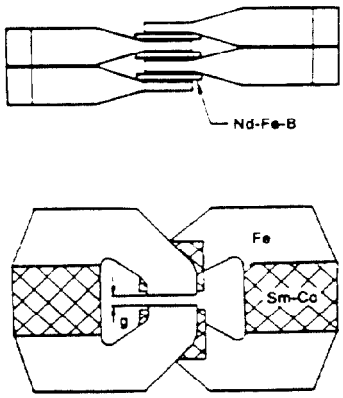

Figure 2. The Kurchatov hybrid undulator (g = 5mm).

5mm. The complete undulator was measured and yielded an average peak field on axis of 6.6kGauss. A computer simulation using the TOSCA[5] code gave similar results. The deviation of the peak field within the undulator has been controlled within a tolerance of 0.5%.

Fig. 3 shows the measured values of the perpendicular magnetic field as measured along the undulator's axis. The 600mm end includes a compensating taper by tilting the endmost Nd-Fe-B magnets 45°. The zero millimeter end shows the field distribution without this compensation.

The first phase of construction consists of this single 60cm undulator section. The second phase of construction will have two separate 60cm undulator sections with a dispersive array installed in between the other sections. The dispersive section provides a shorter distance for the velocity modulation induced by the first section to enhance the bunching of the electron stream in the ponderomotive well.[6]

IV. ELECTRON BEAM DIAGNOSTICS

A. Current and Position:

The electron beam position diagnostic is based upon a design used on ATF at BNL. Each monitor consists of four stripline electrodes placed symmetrically around the electron beam, inside and electrically isolated from the vacuum vessel via ceramic, vacuum feed throughs. The total signal induced on the four striplines is proportional to the total charge in a bunch. The difference of the signals between two diametrically opposed striplines determines the relative position of the

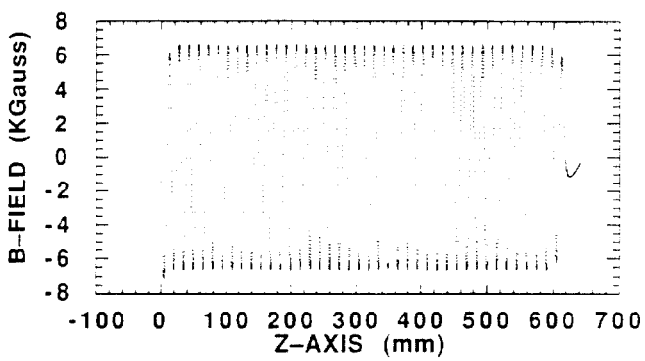

Figure 3. Measured B-field configuration along the axis of the Kurchotov undulator.

electron bunch from the geometric center of the four striplines. The sum and difference signals are subsequently sent to a heterodyne receiver with local oscillator at 2.856GHz, in order to rectify the signal sent to the preamplifier. Each microbunch generates a positive and negative signal of equal magnitude on the electrode, separated by twice the transit time of the electrode's length (i.e., 500psec).[7] The heterodyning process reverses the polarity of the second pulse, therefore the net integrated charge is doubled instead of cancelled in the preamp.

B. Emittance, Energy Spread, and Overall Energy:

Accurate measurements of the electron beam properties are important to understand the FEL behavior. The beam emittance will be measured using a technique similar to that developed at ATF.[8] A phosphor screen is placed to intercept the electron beam. The spot size is reflected into an optical camera. The emittance can be unfolded from the comparison of the spot sizes at two different settings of the beam transport system.[9]

In the dispersive region between two dipole magnets, the energy and energy spread of the electron beam can be measured by placing the phosphour screen at the the beam focus. Since the beam emittance is expected to be low, an angular spread in the spot size at the focus (as seen on the charge-coupled camera viewing the phosphour screen) can by and large be attributed entirely to the energy spread in the beam. The average energy of the beam can be determined from locating the centroid of the electron spot as seen on the phosphour screen and comparing to the calculated trajectory.

C. Temporal Pulse Duration:

The time duration of the electron pulse will be measured by passing the electron beam through a thin plate of dielectric material, then sweeping the Cerenkov radiation thereby produced, on the picosecond time scale using a streak camera.

V. REFERENCES

[1] K. Batchelor, H. Kirk, J. Sheehan, M. Woodle, and K. McDonald, *Proc. European Particle Accel. Conf.*, Rome, Italy, June 7-12, 1988; also, K. Batchelor, *et al.*, *Proc. 1989 Particle Accel. Conf.*, Chicago, IL, p. 273.

[2] C. Pellegrini, *Nucl. Instr. & Meth. Phys. Res.* **A272** (1988) 364.

[3] J. Smolin, T. Katsouleas, C. Joshi, P. Davis, C. Pellegrini, "Design of a plasma wakefield accelerator experiment at UCLA," *Bul. Am. Phys. Soc.* to be publ. Nov. 1990. Cf., T. Katsouleas, J.J. Su, W.B. Mori, C. Joshi, J.M. Dawson, "A compact 100MeV accelerator based on plasma wakefields," *Microwave and Particle Beam Sources and Directed Energy Concepts*, H.E. Brandt, ed., Proc. SPIE 1061, pp. 428-433 (1989).

[4]T.M. Tran and J.S. Wurtele, "Free-electron laser simulation techniques," *Physics Reports* **195** (1990) 1-21.

[5]IEEE Proc. Vol. 127, Pt. B, No. 6 (1980).

[6]J. Gallardo and C. Pellegrini, *Optics Comm.*, **77** (1990) 45.

[7]K.-Y. Ng, "Fields, Impedances, and Structures," in *Phys. of Part. Accelerators*, Vol. One, eds., M. Month and M. Dienes, AIP Conf. Proc. No. 184 (Am. Inst. of Physics, New York, 1989), pp. 472-524; especially §4.3 on beam position monitors.

[8]D.P. Russell, and K.T. McDonald, "A beam-profile monitor for the BNL Accelerator Test Facility (ATF)," *Proc. 1989 IEEE Particle Accel. Conf.*, Vol. 3, eds., F. Bennett and J. Kopta, Chicago, IL., pp. 1510-1512.

[9]K.T. McDonald and D.P. Russell, "Methods of Emittance Measurement," in the *Proc. of the Jont US-CERN School on Observation, Diagnosis and Correction in Part. Beams*, Capri, Italy, October 20-26, 1988.